

Identification of distributed material properties using measured modal data

H. Sol*, T. Lauwagie**, P. Guillaume*

*Vrije Universiteit Brussel (VUB)

Department Mechanics of Materials and Constructions (MEMC), Brussels, Belgium

e-mail: <mailto:hugos@vub.ac.be>

**KULeuven, Departement of Mechanical engineering (PMA),

Celestijnenlaan, 300B, B3001-, Heverlee, Belgium

e-mail: <mailto:Tom.lauwagie@mech.kuleuven.ac.be>

Abstract

Beams, made in brittle materials like concrete or cement, show increasing crack development during their service life due to mechanical and environmental loadings. This local damage can often be translated into reduction of the local bending stiffness values. This paper presents a scanning method to identify the local stiffness values of thin beams using experimentally measured resonance frequencies and their associated mode shapes. A measured modal displacement field is scanned by a special purpose finite beam element. Unlike traditional finite beam elements, each nodal point has the transversal beam deflection as the only degree of freedom (no rotational degrees of freedom). This sole degree of freedom can be compared directly with the measured transversal deflections of mode shapes by a laser Doppler scanner.

The performance of the scanning method is first tested on simulated finite element and experimental data.

1 Introduction

The ability to monitor a structure and detect damage at the earliest possible stage is of outmost importance in civil, mechanical and aerospace engineering communities. Commonly used damage-detection methods are either visual or localized experimental methods such as acoustic or ultrasonic methods, magnetic field methods, radiograph, eddy-current methods and thermal field methods (Doherty [1]). All of these experimental techniques require that the vicinity of the damage is known a priori and that the portion of the structure being inspected is readily accessible. Subjected to these limitations, these experimental methods can detect damage on or near the surface of the structure. The need for additional global damage detection methods that can be applied to complex structures has led to the development and continued research of methods that examine changes in the vibration characteristics of the structure.

Many constructions show increasing crack development during their service life due to mechanical and environmental loadings. This damage can be translated into a modification of mass, damping and stiffness. A vast amount of

methods exists that examine changes in measured vibration response to detect, locate, and characterize damage in structural and mechanical systems. The basic idea behind these methods is that modal parameters (notably frequencies, mode shapes, and modal damping) are functions of the physical properties of the structure (mass, damping, and stiffness). Therefore, changes in the physical properties will cause detectable changes in the modal properties. Literature overview of damage Identification methods using vibration analysis is given, among others, by (Doebling, et al. [2]), (Farrar, et al. [3], [4], [5]), (Rytter [6]).

For beams, plates and shells, there is a direct relationship between curvature and bending strain. The practical issues of measuring strain directly or computing it from displacements or accelerations are discussed by some researchers. (Pandey, et al. [7]) demonstrate that absolute changes in mode shape curvature can be a good indicator of damage for the FEM beam structures they consider. (Stubbs, et al. [8]) present a method based on the decrease in modal strain energy between two structural DOF, as defined by the curvature of the measured mode shapes. (Chance, et al. [9]) found that numerically calculating curvature from mode

shapes resulted in unacceptable errors. They used measured strains instead to measure curvature directly, which dramatically improved results. (Chen and Swamidass [10]), (Dong, et al. [11]), (Kondo and Hamamoto, [12]), and (Nwosu, et al. [13]) present other studies that identify damage and its location from changes in mode shape curvature or strain-based mode shapes.

(Cornwell, et al, [14]) presented a method for damage identification using the concept of strain energy. The method was originally developed for beam-like structures and next further extended for damage identification in plate-like structures. The method only requires the mode shapes of the structure before and after damage. The modes need not to be mass matrix normalised.

Damage typically is a local phenomenon. It is therefore generally accepted that local response is captured best by higher frequency modes whereas lower frequency modes tend to capture the global response of the structure and are less sensitive to local changes in a structure. From a testing standpoint it is more difficult to excite the higher frequency response of a structure as more energy is required to produce measurable response at these higher frequencies than at the lower frequencies (Doebling, et al. [2])

This paper discusses a method to identify damage by evaluating the distributed stiffness values in a simple beam according to the Euler-Bernoulli (EB) equations. The presented method will use both resonance frequency and mode shape information. The mode shapes need not to be mass normalised. Output only modal analysis can hence be used. The method is a linear, model based, inverse method and aims the determination of the location and quantification of the beam stiffness. It is proved that the information contents of only the first bending mode shape is sufficient for the identification of a complete stiffness pattern.

The differential equation describing the deflections of a EB-beam can be found in many text books about strength of materials and constructions (Seed, [15]):

$$\frac{d^2}{dx^2} (EI \frac{d^2 w(x)}{dx^2}) = p(x) \quad (1)$$

In the above expression w is the local beam deflection, x is the independent spatial variable, E is the Young's modulus, I is the moment of inertia of the beam's cross section and p is the distributed pressure. The product EI is called the flexural beam rigidity and its value can be an arbitrary function of the independent variable x .

Identification of the value of parameters occurring in differential equations (like EI in (1)) can be performed in geometrical three different regions of the considered domain:

1. In one arbitrary point
2. In the whole domain
3. In an arbitrary sub domain

The value of the parameters can be different in each point of the (sub)domain and the problem hence can be referred to as "the identification of distributed parameter values".

1.1. One point identification

The identification of EI using a one point method uses directly the differential equation in the considered point:

$$EI(x_i) \frac{d^4 w(x_i)}{dx^4} = p(x_i) \quad (2)$$

$$EI(x_i) = \frac{p(x_i)}{\frac{d^4 w(x_i)}{dx^4}} \quad (3)$$

The evaluation of EI in a single point x_i requires the knowledge of $p(x_i)$ and the fourth derivative of the deflection w . Due to inevitable measurement noise, the experimental evaluation of (higher order) derivatives of the beam deflection is a difficult task and requires some previous curve fitting of the measured deflections. The problem can be simplified by using e.g. the relation of the bending moment with the second derivative of the deflection (Maeck, et al. [16]).

1.2. Whole domain identification

The identification of EI as a distributed parameter over the whole beam length can be considered as a global parameter estimation problem. As an analytical model for a beam with arbitrary distributed stiffness values is not available, a numerical model (e.g. a finite element model) must be adopted. Updating of a numerical model can be performed using an inverse method.

The principle of a mixed numerical/experimental method or "an Inverse method" for material parameter identification is to compare a measured output from an experiment on a test specimen with the computed output of a numerical model of the same specimen loaded with the same input values. (Sol [17])

An input can be some force distribution. An output can be a static or dynamic displacement, stress or strain field. It can also be a list of quantities

derived from the beam response like resonance frequencies, mode shapes and associated damping ratios.

The difference between the measured and computed output is called "the residual". The residual can be incorporated in a user defined cost function that describes the goodness of fit of the numerical model with the test specimen. A simple example of a cost function is the summation of the squared differences between the corresponding output components.

The - a priori unknown - distributed beam stiffness values EI are the parameters in the numerical model. The complete set of distributed beam stiffness values is (usually iteratively) tuned in such a way that the computed output matches the measured output. The parameter modifications are computed by minimisation of the cost function. The final result of the output matching procedure is an estimate of the parameters values and eventually an estimate of their error bounds. Modal quantities like resonance frequencies and mode shapes are often used as measured output values (Friswell [17]).

The main advantages of using modal quantities instead of static deflections is that the experimental set-ups are easy and that -with modern equipment and software- the modal quantities can be measured fast and accurate.

A major disadvantage of a whole domain identification method is the considerable computation time that is necessary to perform an iterative procedure with FE-models having a high number of dof's..

1.3 Sub domain identification

Sub domain identification applies the same idea as the inverse methods on a sub domain of the considered construction instead of on the whole construction domain. The difficulty with sub domain identification is that the appropriate boundary conditions on the sub domain need to be determined. The boundary conditions must be such that they represent the action of the remaining parts of the considered domain on the boundaries of the selected sub domain. The sub domain can be hence isolated without changing the stress state conditions in arbitrary points of the sub domain

In the next chapter the idea of applying sub domain identification on beams will be explored. The beam stiffness will be identified ("scanned") in an arbitrary number of beam segments.

2 Distributed Stiffness Scanning

2.1. Integral formulation

Consider a beam vibrating in resonance at a circular frequency ω . The transverse displacements of the associated mode shape are $w(x,t)$. The partial differential equation of the equilibrium in an arbitrary point in the domain of the resonating beam is:

$$\frac{\partial^2}{\partial x^2} (EI(x) \frac{\partial^2 w(x,t)}{\partial x^2}) + rA(x) \frac{\partial^2 w(x,t)}{\partial t^2} = 0 \quad (4)$$

In the above expression x is the independent spatial variable, t is the independent time variable, E is the Young's modulus, I is the moment of inertia of the beam's cross section, ρ is the specific mass and A is the area of the beam's cross section. The product EI is the flexural rigidity or "stiffness" of the beam cross section. The product ρA is the mass per unit length of the beam. EI and ρA can be both arbitrary functions of the independent variable x .

The solution of (4) written in imaginary notation is (splitting of the function $w(x,t)$ into a product of functions with independent variables) at a beam resonance:

$$w(x,t) = W(x) \cdot e^{i\omega t} \quad (5)$$

with ω the circular frequency of the beam resonance mode and $W(x)$ the arbitrary scaled modal deformation term.

Thus:

$$\frac{\partial^2 w}{\partial t^2} = -\omega^2 W(x) \cdot e^{i\omega t} \quad (6)$$

Substitution of this solution transforms the equation (4) in a time independent normal differential equation:

$$\frac{d^2}{dx^2} (EI(x) \frac{d^2 W(x)}{dx^2}) - rA \omega^2 W(x) = 0 \quad (7)$$

(7) can be seen as the differential equation of a beam loaded statically with a distributed pressure $p(x) = rA \omega^2 W(x)$.

Consider a small beam segment in the interval $[x_k, x_l]$. The segment is sufficiently small to assume constant flexural rigidity EI and constant mass per unit length ρA . (7) for the beam segment hence simplifies to:

$$EI \frac{d^4 W(x)}{dx^4} - rA \omega^2 W(x) = 0 \quad (8)$$

The beam segment is in each of the two boundary points x_k and x_l subjected to prescribed transversal displacements $(\bar{W}_k$ and $\bar{W}_l)$ as Dirichlet

boundary conditions and prescribed bending moments (\bar{M}_k and \bar{M}_l) as Von Neumann boundary conditions.

The differential equation (8) must be satisfied in each point of the beam domain. In addition, solutions of (8) must satisfy the boundary conditions of the beam at points x_k and x_l .

The local formulation (8) can be transformed into an equivalent global formulation having the same solution for the dependant variable W . This transformation can be performed by using the weighted residual method with a virtual displacement field $\delta V(x)$ as weighting function for the differential equation, and V_k and V_l as arbitrary weighting scalars for the Von Neumann boundary conditions. The Dirichlet boundary conditions will be introduced explicitly in a latter stage. The virtual displacement field can be taken zero at the two boundaries because the Dirichlet conditions are explicitly imposed at these positions.

The global formulation hence becomes:

$$\int_{x_k}^{x_l} EI \frac{d^4 W}{dx^4} dV dx - \int_{x_k}^{x_l} rAw^2 W dV dx + (EI \frac{d^2 W}{dx^2} - \bar{M}_k) V_k + (EI \frac{d^2 W}{dx^2} - \bar{M}_l) V_l = 0 \tag{9}$$

Partial integration of the first term of (9) gives:

$$\left[EI \frac{d^3 W}{dx^3} dV \right]_{x_k}^{x_l} - \int_{x_k}^{x_l} EI \frac{d^3 W}{dx^3} \cdot \frac{dV}{dx} dx - \int_{x_k}^{x_l} rAw^2 W dV dx + (EI \frac{d^2 W}{dx^2} - \bar{M}_k) V_k + (EI \frac{d^2 W}{dx^2} - \bar{M}_l) V_l = 0 \tag{10}$$

The first term of (10) vanishes because the virtual field δV has a zero value in the boundary points x_k and x_l .

A second partial integration leads to:

$$- \left[EI \frac{d^2 W}{dx^2} \frac{dV}{dx} \right]_{x_k}^{x_l} + \int_{x_k}^{x_l} EI \frac{d^2 W}{dx^2} \cdot \frac{d^2 V}{dx^2} dx - \int_{x_k}^{x_l} rAw^2 W dV dx + (EI \frac{d^2 W}{dx^2} - \bar{M}_k) V_k + (EI \frac{d^2 W}{dx^2} - \bar{M}_l) V_l = 0 \tag{11}$$

Select the following values for V_k and V_l (so far V_k and V_l were completely arbitrary):

$$V_k = \frac{dV}{dx}(x_k) \tag{12}$$

$$V_l = - \frac{dV}{dx}(x_l)$$

(11) becomes:

$$EI \int_{x_k}^{x_l} \frac{d^2 W}{dx^2} \cdot \frac{d^2 V}{dx^2} dx = \int_{x_k}^{x_l} rAw^2 W dV dx + \bar{M}_k \cdot \frac{dV}{dx}(x_k) - \bar{M}_l \cdot \frac{dV}{dx}(x_l) \tag{13}$$

2.2 Finite element approximation

The considered beam segment interval $[x_k, x_l]$ is divided into a regular grid of M nodal points. The transversal displacement amplitude $W(x)$ is expressed as a linear combination of Lagrange shape functions N_i multiplied with the value of $W(x)$ in the nodes. Each node i is associated with a shape function N_i and has only one degree of freedom W_i .

$$W(x) = N_i(x) \cdot W_i \tag{14}$$

Because the integral in (13) is a symmetrical expression, the virtual field δV can be expressed with the same interpolation functions N_i :

$$dV(x) = N_i(x) \cdot dV_i \tag{15}$$

with $\delta V_k = 0$ and $\delta V_M = 0$ at the boundary nodes.

Lagrange shape functions N_i of order M are selected:

$$N_i(x) = \frac{(x-x_1)(x-x_2)\dots(x-x_{i-1})(x-x_{i+1})\dots(x-x_M)}{(x_i-x_1)(x_i-x_2)\dots(x_i-x_{i-1})(x_i-x_{i+1})\dots(x_i-x_M)} \tag{16}$$

The shape functions of node i have the value 1 in node $x = x_i$ and the value zero in all other nodal points $x = x_j$ ($i \neq j$).

Insertion of (14) and (15) in (13) and the requirement that (13) must be valid for each arbitrary virtual field, yields the following expression:

$$EI \int_{x_k}^{x_l} \frac{d^2 N_i}{dx^2} \cdot \frac{d^2 N_j}{dx^2} dx \cdot W_j = rAw^2 \int_{x_k}^{x_l} N_i N_j dx \cdot W_j + \bar{M}_k \cdot \frac{dN_i}{dx}(x_k) - \bar{M}_l \cdot \frac{dN_i}{dx}(x_l) \tag{17}$$

$i = 2, 3, \dots, M-1$
 $j = 1, 2, \dots, M$

The first terms on each side of the equations can be called respectively "stiffness matrix" K_{ij} and "mass matrix" M_{ij} of the considered beam element.

$$K_{ij} = EI \int_{x_k}^{x_l} \frac{d^2 N_i}{dx^2} \cdot \frac{d^2 N_j}{dx^2} dx \tag{18}$$

$$M_{ij} = rAw^2 \int_{x_k}^{x_l} N_i N_j dx$$

[K] and [M] are non square rectangular matrices because the indices i and j take other values. Because the transversal displacement W is the only degree of freedom in the nodes, the formulation can not be used as a standard finite element formulation. The assemblage of standard thin beam finite elements requires indeed C1-continuity in the boundary nodes which can only be guaranteed with the introduction of an extra rotational degree of

freedom in the nodes. The proposed element formulation (18) however will never be assembled and hence requires no inter-element C1-continuity.

It is convenient for programming purposes to replace the Cartesian coordinate x by a local homogenised coordinate ξ ?

$$\mathbf{x} = \frac{2(x - \frac{x_l + x_k}{2})}{x_l - x_k} = \frac{2(x - \frac{x_l + x_k}{2})}{L^e} \quad (19)$$

$$dx = \frac{L^e d\mathbf{x}}{2}$$

with L^e the length of the considered segment.

(17) written in homogenised coordinates ξ becomes:

$$\frac{8EI}{L^e{}^3} \int_{-1}^1 \frac{d^2 N_i}{d\mathbf{x}^2} \cdot \frac{d^2 N_j}{d\mathbf{x}^2} \cdot d\mathbf{x} \cdot W_j = \quad (20)$$

$$\frac{\mathbf{r}A\mathbf{w}^2 L^e}{2} \int_{-1}^1 N_i N_j \cdot d\mathbf{x} \cdot W_j + \frac{2\bar{M}_k}{L^e} \cdot \frac{dN_i}{d\mathbf{x}}(-1) - \frac{2\bar{M}_l}{L^e} \cdot \frac{dN_i}{d\mathbf{x}}(1)$$

The integrals in (20) have become independent on the size and properties of the considered beam interval. The Lagrange shape functions are now expressed as functions of the independent variable ξ :

$$N_i(\mathbf{x}) = \frac{(\mathbf{x} - \mathbf{x}_1)(\mathbf{x} - \mathbf{x}_2) \dots (\mathbf{x} - \mathbf{x}_{i-1})(\mathbf{x} - \mathbf{x}_{i+1}) \dots (\mathbf{x} - \mathbf{x}_M)}{(\mathbf{x}_i - \mathbf{x}_1)(\mathbf{x}_i - \mathbf{x}_2) \dots (\mathbf{x}_i - \mathbf{x}_{i-1})(\mathbf{x}_i - \mathbf{x}_{i+1}) \dots (\mathbf{x}_i - \mathbf{x}_M)} \quad (21)$$

Pre-multiplying both sides of equation (20) with W_i allows to evaluate EI as a function of W_i , boundary conditions and known beam parameters:

$$EI = \frac{\mathbf{r}A\mathbf{w}^2 L^e{}^4 B_{ij} W_i W_j + 4L^e{}^2 \bar{M}_k W_i \frac{dN_i}{d\mathbf{x}}(-1) - 4L^e{}^2 \bar{M}_l W_i \frac{dN_i}{d\mathbf{x}}(1)}{16A_{ij} W_i W_j} \quad (22)$$

with:

$$A_{ij} = \int_{-1}^1 \frac{d^2 N_i}{d\mathbf{x}^2} \cdot \frac{d^2 N_j}{d\mathbf{x}^2} \cdot d\mathbf{x}$$

$$B_{ij} = \int_{-1}^1 N_i N_j \cdot d\mathbf{x}$$

$$i = 2, 3, \dots, M - 1$$

$$j = 1, 2, \dots, M \quad (23)$$

The evaluation of (22) hence requires the values of W_i in all the points of the selected beam segment and the values (\bar{M}_k and \bar{M}_l) at the boundaries of the segment.

3 Identification of distributed beam stiffness values by a scanning element method

3.1 Determination of the reduction elements

Consider again a free-free beam vibrating in resonance at a circular frequency ω . The time

independent differential equation describing the geometry of the mode shape $W(x)$ is (7):

$$\frac{d^2}{dx^2} (EI(x) \frac{d^2 W(x)}{dx^2}) - \mathbf{r}A(x) \mathbf{w}^2 W(x) = 0 \quad (7)$$

(7) can be seen as the differential equation of a beam loaded statically with a distributed pressure $p(x) = \mathbf{r}A\mathbf{w}^2 W(x)$. The pressure distribution is such that the load causes no rigid body translation or rotation. This is obvious as the origin of the pressure distribution is a mode shape of a free-free beam. (7) can be rewritten as;

$$\frac{d^2}{dx^2} (EI \frac{d^2 W(x)}{dx^2}) = p(x)$$

$$p(x) = \mathbf{r}A\mathbf{w}^2 W(x) \quad (24)$$

Integration of equation (25) gives:

$$\frac{d}{dx} (EI \frac{d^2 W(x)}{dx^2}) = Q(x)$$

$$Q(x) = \int_0^x p(V) dV \quad (25)$$

$Q(x)$ is the transverse shear force at position x . In case of a free-free beam with length L , the shear force is zero at the beam boundaries $x=0$ and $x=L$.

Integration of equation (25) gives:

$$EI \frac{d^2 W(x)}{dx^2} = M(x)$$

$$M(x) = \int_0^x Q(V) dV \quad (26)$$

$M(x)$ is the bending moment at position x . In case of a free-free beam with length L , the bending moment is zero at the beam boundaries $x=0$ and $x=L$.

3.2 Principle of stiffness scanning

If one wants to know the stiffness distribution of a test beam, the first step is to experimentally measure a resonance frequency and an associated mode shape. Modern equipment allows to measure the mode shapes in a high number of points N . The measured modal amplitudes have the same degree of freedom as the only degree of freedom in the described scanning finite element. The experimental

and numerical amplitudes can hence be directly compared with each other.

In the previous paragraph it was shown that it is possible to derive the reduction elements $Q(x)$ and $M(x)$ starting from the knowledge of the resonance frequency and the associated mode shape $W(x)$.

A second step in the identification procedure is to evaluate $M(x)$ in the N measurement points. After this step, all information is available to apply formula (22) to identify the beam stiffness EI .

The total beam length can be divided in an arbitrary number of discrete beam segments each containing M consecutive measurement points.

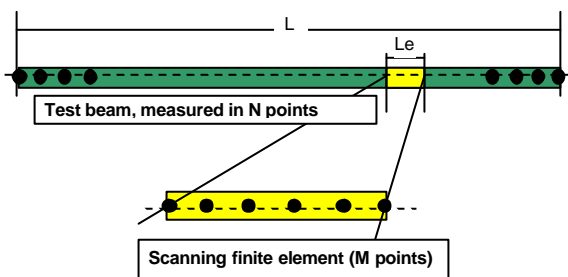


Figure 1: Principle of the scanning element

The M nodal points of the scanning element are associated with the M consecutive points of the selected beam segment L_e (see Figure 1). The beam stiffness in the segment is assumed to be constant. The stiffness of the beam segment can be identified using the experimentally measured displacements and computed boundary conditions. Using formula (22), the stiffness value EI of an arbitrary interval of the beam can be identified.

Starting from the left of the test beam and progressing to the right, all measured displacements can be associated in groups of M measurement points to the M nodal points of the scanning element. In each position, the scanning element can identify the beam stiffness of the considered beam segment.

3.3. Validation on simulated test examples

The commercial finite element program ANSYS is used to generate some test examples. The first example is a beam with a constant cross section A , a constant specific mass ρ , a constant inertia moment I and a constant Young's modulus E .

A first test beam was given following properties:

BEAM GEOMETRY INFORMATION:

- Beam length [m]: .2000E+00
- Beam width [m]: .1200E-01
- Beam thickness [m]: .2000E-02

BEAM PROPERTIES INFORMATION:

- Specific weight [kg/m**3]: .2800E+04
- Cross sectional area [m**2]: .2400E-04
- Beam inertia moment [m**4]: .8000E-11
- Young's modulus [N/m**2]: .7000E+11
- Beam stiffness [Nm]: .5600E+00

The first computed frequency by ANSYS was 256.93 Hz using a model with 50 beam elements and 51 nodes. The computed associate bending mode shape was used to perform a scan with $M = 4$ points (Figure 3.3.1):

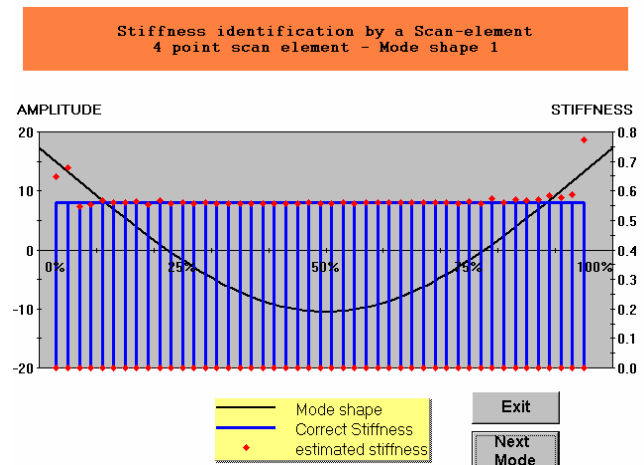


Figure 2: Stiffness distribution estimation using the first mode shape.

A second test beam was given a linear varying Young's modulus:

BEAM GEOMETRY INFORMATION:

- Beam length [m]: 1.00
- Beam width [m]: .100
- Beam thickness [m]: .010

BEAM PROPERTIES INFORMATION:

- Specific weight [kg/m**3]: .2500 E+04
- Cross sectional area [m**2]: .1000 E-02
- Beam inertia moment [m**4]: 8.33 E-09
- Young's modulus [N/m**2]: from .5000E+11 till .7000E+11
- Beam stiffness [Nm]: from 383.4 till 583.4

The first computed frequency by ANSYS was 46.503 Hz using a model with 50 beam elements and 51 nodes. The computed associate bending

mode shape was used to perform a scan with $M = 4$ points (see Figure 3):

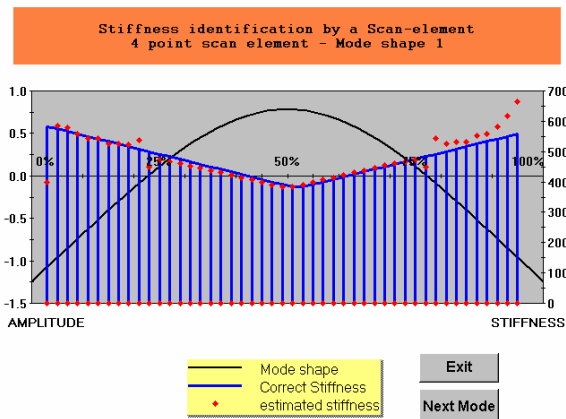


Figure 3: Stiffness distribution estimation using the first mode shape.

3.3.4 Discussion of the results

It can be seen in figure 2 that the (known) constant beam rigidity can be found back nearly correct using the scanning element technique. The stiffness in the beam intervals close to the free boundaries of the beam could not be identified because the mode shape does not have sufficient curvature at both extreme ends (and hence contains no information of the stiffness behaviour).

The observations for the beam with linear varying stiffness (figure 3) are similar.

The results are not "perfect" because the displacement field obtained with the finite element method is piecewise linear varying and thus not continuous.

4 Experiments

The scan element method is tested on beam specimens made in glass fibre reinforced IPC (Inorganic phosphate cement). IPC is a cementitious matrix material used in sandwich constructions (Wastiels [19]). The properties of the IPC beam are:

- Length [m]: 0.213
- Width [m]: 0.0195
- Thickness [m]: 0.005
- Mass [kg]: 0.036

An experimental modal analysis is first carried out on an undamaged IPC beam. From this analysis the natural frequencies and mode shapes of the beam are obtained. The scan element technique is next used to establish the stiffness distribution of the undamaged beam.

After characterisation of the undamaged beam, the specimen is increasingly damaged by a controlled

three point bending and the scan procedure is repeated.

4.1. Experimental modal analysis

The composite IPC beam is suspended on very soft elastic cords in order to approximate the free-free boundary conditions.



Figure 5: Experimental test set-up with the suspended IPC test beam.

Figure 5 shows the suspended IPC test beam. The beam is excited acoustically with a small loudspeaker. The excitation signal used is a periodic chirp with an amplitude of 1 Volt. A periodic chirp is a very rapid sine sweep with a frequency swept up and/or down in one observation period of data acquisition. The procedure repeats this sweeping and thus the excitation signal becomes a periodic function. All frequencies of the test beam lying in the used bandwidth of the periodic chirp are excited simultaneously. In the test, the bandwidth is from 100 Hz till 10 kHz. The excitation signal is multiplied with a rectangular window function. The window cuts off the time signal outside the time window. An acoustical excitation is used in order to avoid physical contact of the excitation source with the test beam. An electro magnetic shaker would have a notable influence on the light weight test beam. A disadvantage of this technique is that the input force can not be measured (output only modal analysis "OMA").

A polytec Scanning Vibrometer (PSV) using a laser beam is used to measure the response of the beam to the excitation signal. The PSV is a full-field system for automated vibration measurement, mapping, visualization and analysis. It measures the velocity of points on a vibrating structure. Measurements are made point by point in a scanning mode. The laser beam is a non-contacting transducer and avoids the problem of mass loading.



Figure 6: The scan head of the PSV (Polytechnic Scanning Vibrometer)

The scan head of the PSV (Figure 6) contains deflection mirrors, a live colour video camera and a Laser Doppler Velocity sensor. The deflection mirrors automatically steers the laser beam to the desired position on the target. The live video camera displays the laser beam on the target and allows the user to draw a grid of desired measurement points right over a video image. After every measurement, the area data are conveniently overlaid directly upon the video image.

The scanning area of the laser beam is defined by 4 calibration points. The area is divided into a regular grid of 3 rows (width of the beam) and 213 columns (length of the beam). 639 measurement points are hence obtained yielding a spatial resolution of 1 mm in the length of the test beam.

The software to analyse the experimental data is CADA-X v. 3.5C from the company LMS.

4.2. Modal Analysis on the undamaged beams

Figure 7 shows the obtained mode shape for the first bending mode of the IPC test beam.

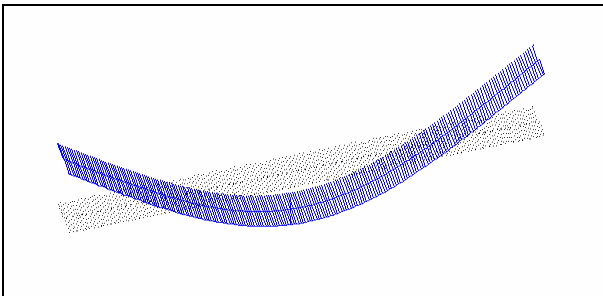


Figure 7: first bending mode shape at 296.43 Hz (measured with PSV in 3 x 213 points)

4.3. Data pre-processing

Experimental data usually contains a vast amount of noise. Due to the presence of this noise, the measured raw data can not be used directly (as was possible with the "smooth" finite element simulations). The raw data was smoothed by fitting the experimental data with a 10th degree Lagrange polynomial

The free-free boundary conditions of the test beam require a translational and rotational equilibrium. If this is not the case, the shear force and the bending moment computed with equations (5) and (6) will not be zero at $x = L$.

Deviations from these equilibrium conditions can occur due to experimental errors, the curve fit procedure and the integration procedure.

In order to impose translational and rotational equilibrium, the curve fitted results are superposed by two rigid body modes: a pure translation and a pure rotation in $x=L/2$.

$$W(x)_{corrected} = W(x)_{fitted} + a.W(x)_{translation} + b.W(x)_{rotation}$$

with:

$$W(x)_{translation} = 1$$

$$W(x)_{rotation} = \frac{2x}{L} - 1 \quad (27)$$

The requirements are:

$$Q(x=L) = \int_0^L W_{corrected}(x) dx = 0 \quad (28)$$

$$M(x=L) = \int_0^L x.W_{corrected}(x) dx = 0 \quad (29)$$

The parameters a and b in (27) must be determined in such a way that the requirements (28) and (29) are fulfilled. This leads to:

$$a = -\frac{Q(x=L)}{w^2 rAL} \quad (30)$$

$$b = -\frac{6M(x=L)}{w^2 rAL^2} - 3a$$

In the above expression, Q and M are computed with the previously computed curve fitted data.

4.4. Stiffness identification of the undamaged test beam

The 3 measured values in each row of the CADA-X data were averaged so that 213 actual experimental points were used for the damage scanning.

The measured first mode shape of the undamaged IPC beam was curve fitted with the Lagrange polynomial. A $M=7$ point scanning element was used for the damage identification. Taking less nodal points made the obtained damage pattern

more "nervous", more nodal points resulted in a loss of detail.

The coefficients for the rigid body corrections computed with (30) are:

$$\begin{aligned} \text{coefficient a:} & \quad .2315\text{E-}02 \\ \text{coefficient b:} & \quad .9864\text{E-}02 \end{aligned}$$

Figure 8 shows the identified stiffness pattern in the undamaged beam

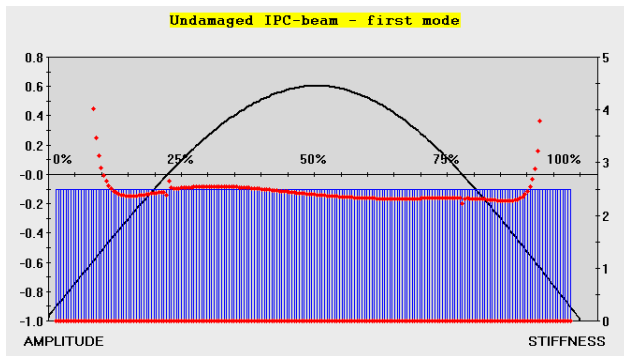


Figure 8: Identified stiffness distribution in an undamaged IPC beam

In figure 8, the blue lines show the constant beam stiffness values computed with the resonance frequency of the first mode shape (2.49 Nm²). The thick red line is the identified local stiffness distribution. As can be seen, the stiffness of the undamaged beam is not perfectly constant. This is probably due to small variations in thickness and initial local material properties. It can also be seen that the stiffness values identified in the zone of approximately 15% of the free ends of the beam are not useful. This is due to the lack of curvature (and hence information contents) of the observed mode shape in these zones.

4.5. Stiffness identification of the damaged test beam

The test beam was damaged in a controlled way using a 3 point bending set-up and a force of 54 Newton. Figure 9 shows the result using the same number of nodal points scan element (M=7).

Conclusions

The thin beam scanning finite element with only one degree of freedom is very useful as a tool for direct comparison of measured beam deflections with computed deflections. It was shown in this paper that the mode shape of the first bending resonance frequency has a sufficient information

contents to identify the stiffness distribution in undamaged and damaged beams. Further research will examine suitable curve fitting procedures in order to include higher order mode shapes (which will provide redundant information to compensate for experimental errors). The scanning element procedure will also be extended toward scanning of plate and shell structures.

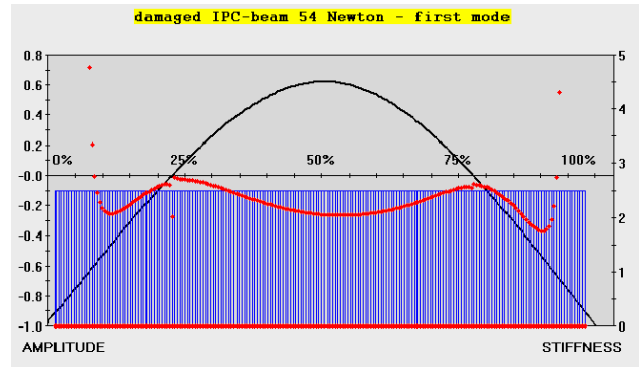


Figure 9: Identified stiffness distribution in a beam damaged with 54 Newton

Acknowledgements

Part of this work was carried out in the framework of the project GRAMATIC, which is financially supported by the Flemish government Institute IWT.

References

- [1] Doherty, J. E., 'Nondestructive Evaluation,' Chapter 12 in Handbook on Experimental Mechanics, A. S. Kobayashi Edt., Society for Experimental Mechanics, Inc., 1987.
- [2] Doebling, S. W., Farrar, C. R., Prime, M. B., and Shevitz, D. W. "Damage Identification and Health Monitoring of Structural and Mechanical Systems from Changes in their Vibration Characteristics: A Literature Review," Los Alamos National Laboratory report LA 13070-MS, april 1996
- [3] Farrar, C.R., Doebling, S.W., and Duffey, T.A., "Vibration-Based Damage Detection," presented at the SD2000 Structural Dynamics Forum, April 11-17, 1999.

- [4] Farrar, C.R. and Doebling, S.W., "An Overview of Modal-Based Damage Identification Methods," in Proc. of DAMAS Conference, Sheffield, UK, June 1997.
- [5] Farrar, C.R., Doebling, S.W., Nix, D.A., 2001, "Vibration-Based Structural Damage Identification," Philosophical Transactions of the Royal Society: Mathematical, Physical & Engineering Sciences, Vol. 359, No. 1778, pp. 131 – 149
- [6] Rytter, A., "Vibration based inspection of civil engineering structures," Ph. D. Dissertation, Department of Building Technology and Structural Engineering, Aalborg University, Denmark, 1993.
- [7] Pandey, A. K., M. Biswas, and M. M. Samman, "Damage detection from changes in curvature mode shapes," Journal of Sound and Vibration, 145(2), 321–332, 1991.
- [8] Stubbs, N., J.-T. Kim, and K. Topole, "An efficient and robust algorithm for damage localization in offshore platforms," in Proc. ASCE Tenth Structures Congress, 543–546, 1992.
- [9] Chance, J., G. R. Tomlinson, and K. Worden, "A simplified approach to the numerical and experimental modelling of the dynamics of a cracked beam", in Proc. of the 12th International Modal Analysis Conference, 778–785, 1994.
- [10] Chen, Y., and A. S. J. Swamidias, "Dynamic characteristics and modal parameters of a plate with a small growing surface crack", in Proc. of the 12th International Modal Analysis Conference, 1155–1161, 1994.
- [11] Dong C., P. Q. Zhang, W. Q. Feng, and T. C. Huang, "The sensitivity study of the modal parameters of a cracked beam", in Proc. of the 12th International Modal Analysis Conference, 98–104, 1994.
- [12] Kondo, I. and T. Hamamoto, "Local damage detection of flexible offshore platforms using ambient vibration measurements", in Proc. of the 4th International Offshore and Polar Engineering Conf., 4, 400–407, 1994.
- [13] Nwosu, D.I., A. S. J. Swamidias, J. Y. Guigne, and D. O. Olowokere, "Studies on influence of cracks on the dynamic response of tubular T-joints for non-destructive evaluation", in Proc. of the 13th International Modal Analysis Conference, 1122–1128, 1995.
- [14] Cornwell, P.J., Doebling, S.W., and Farrar, C.R., 1999, "Application of the Strain Energy Damage Detection Method to Plate-Like Structures", Journal of Sound and Vibration, Vol. 224, No. 2, 359-374.
- [15] Seed, G.M., "Strength of Materials", Saxe Coburg publications, 2000
- [16] Maeck, J., De Roeck, G., "Dynamic bending and torsion stiffness derivation from modal curvatures and torsion rates", Journal of sound and vibration; 225(1), 1999, pp.153-170
- [17] Sol, H., Oomens, C.W.J., "Material identification using mixed numerical experimental methods", Proc. of the Euromech colloquium, Kerkrade, The Netherlands, 7-9 april, 1997
- [18] Friswell, M.E., Mottershead, J.E., "Finite element updating in structural dynamics", Kluwer academic press, 1999 "
- [19] Wastiels, J., "Sandwich panels in construction with HPFRCC-faces: New possibilities and adequate modelling", Proc. of RILEM, Mainz, Germany, May 16-19, 1999